JOURNAL OF MATERIALS SCIENCE **38** (2003) 4129–4135

An investigation of the effects of thickness on mechanical properties of LIGA nickel MEMS structures

J. LOU, S. ALLAMEH
Princeton Materials Institute, Mechanical and Aerospace Engineering Department, Princeton University, Princeton, NJ 08544, USA

T. BUCCHEIT
Mechanical Reliability and Modeling Department, Sandia National Laboratories, Albuquerque, New Mexico, USA

W. O. SOBOYEJO
Princeton Materials Institute, Mechanical and Aerospace Engineering Department, Princeton University, Princeton, NJ 08544, USA

This paper examines the effects of thickness on the mechanical properties of LIGA Ni MEMS structures plated from sulfamate baths. The as-plated LIGA Ni specimens of different thickness (50 μm, 100 μm and 200 μm) were utilized in the microtensile experiments. Optical microscopy, orientation imaging microscopy and scanning electron microscopy were used to characterize the microstructure of the LIGA Ni specimens. Fracture Modes obtained from specimens with different thickness were revealed by scanning electron microscopy. The effects of specimen thickness are then discussed within the context of strain gradient plasticity theories.

1. Introduction

In recent years, LIGA (an acronym of the German words "Lithogrphic, Galvanoformung, Abformung") nickel micro-electro-mechanical systems structures have been developed for applications in larger and thicker devices [1–4]. These include applications in micro-switches [1–4] and accelerometers that are used for the deployment of air bags [1]. In many of these applications, a basic understanding of the deformation mechanisms at the micron scale is critical to the long-term application of LIGA Ni MEMS structures. Since the potential range of thicknesses used in actual Ni MEMS structures is between ~10 μm to ~700 μm, it is essential to understand how the material will behave in this range. However, the possible effects of thickness on the mechanical behavior of LIGA Ni MEMS structure have not been studied in detail.

This paper presents the results of an experimental study of the effects of thickness on the mechanical properties of LIGA Ni structures plated from sulfamate baths. As-plated LIGA Ni specimens of different thicknesses (50, 100 and 200 μm) were utilized in micro-tensile experiments that were used to characterize the constitutive behavior of the LIGA Ni MEMS structures. The microstructures of as-received samples were characterized using optical microscopy, scanning electron microscopy and orientation imaging microscopy. The effects of specimen thickness are then discussed within the context of strain gradient plasticity theories.

2. Material and microstructures

LIGA is an additive microfabrication process in which structural material is deposited into a polymethylmethacrylate (PMMA) molds realized by deep X-ray photolithograpy (DXRL) [5]. The LIGA Ni specimens used in this study were electrodeposited using sulfamate bath chemistry (Table I) at Sandia National Laboratories, Livermore, CA. The details of the fabrication process are outlined by Christenson *et al.* [2].

The microstructure of the as-deposited LIGA Ni specimens was studied using optical microscopy and scanning electron microscopy. The micrographs of transverse cross-sections of the LIGA Ni specimens obtained using optical and electron microscopy are shown in Fig. 1. The micrographs show that as deposited LIGA Ni has a complex hierarchical microstructure. The optical micrograph of the transverse cross-section (shown in Fig. 1a) indicates the presence of predominantly columnar structures oriented parallel to the deposition direction. The columnar structures are approximately 5 μm wide and 5–25 μm long. At higher magnification, the scanning electron micrographs (shown in Fig. 1b–d)

TABLE I Composition and operating conditions of nickel sulfamate plating baths

$Ni((NH_2SO_3)_2 \cdot 4H_2O$	440.1 g/l
Boric acid	48 g/l
Wetting agent	0.2 %/vol
Temperature	50°C
PH	3.8–4.0

0022–2461

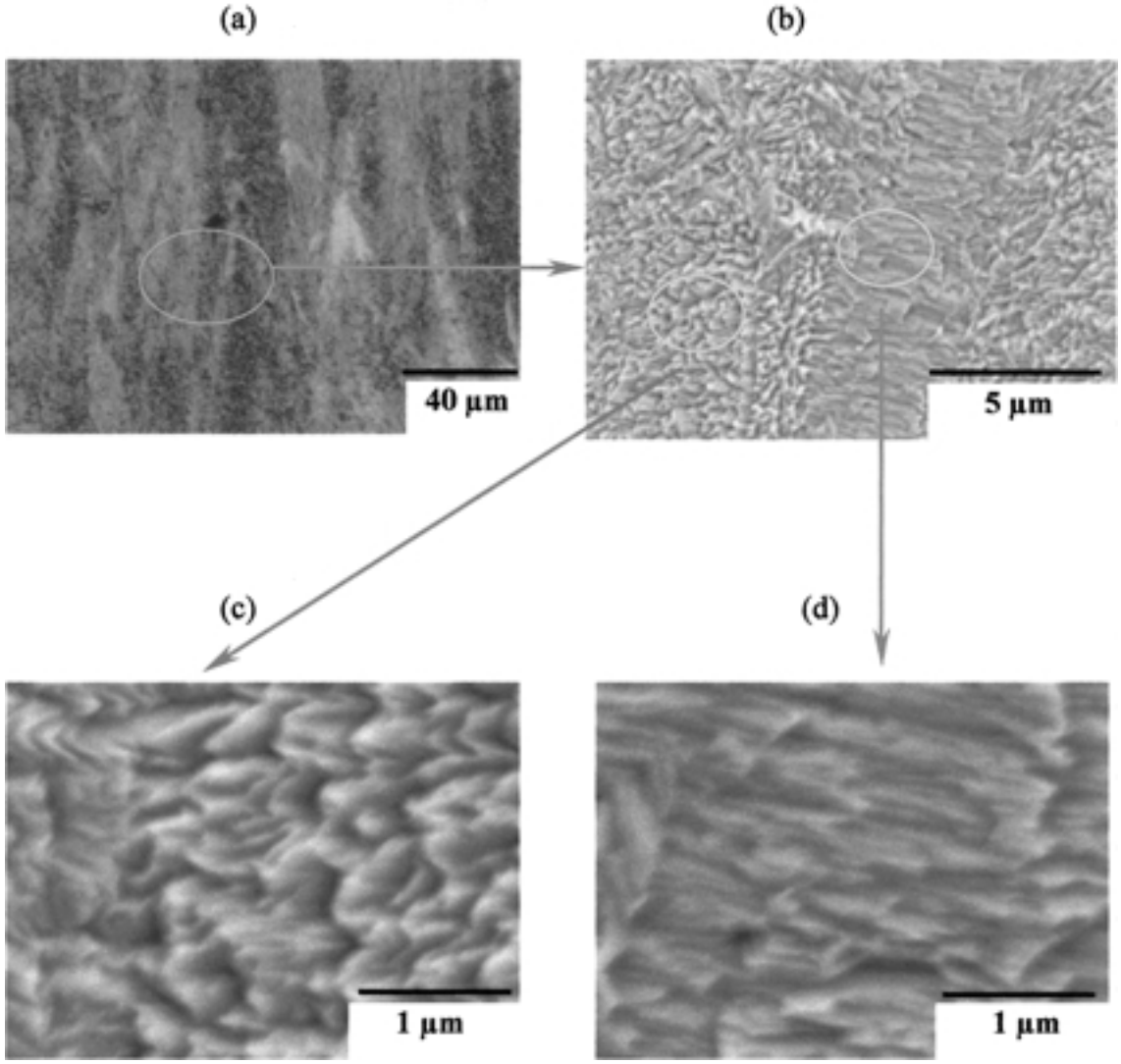

Figure 1 Microstructure of the as-plated LIGA Ni: (a) Optical micrograph of the transverse-cross section, (b) Scanning electron micrograph of the transverse cross-section, and (c)–(d) Scanning electron micrograph showing details of the columnar structure in the transverse cross-section.

reveal that the adjacent columnar structures are composed of needle shaped grains oriented along perpendicular directions in the plane normal to the deposition direction. The grains in each columnar structure are approximately 500 nm long.

Orientation imaging microscopy (OIM) analyses were conducted on cross-sectioned as-received LIGA Ni foil from sulfamate bath as shown in Fig. 2. The predominantly red color in Fig. 2 reveal that a sharp ⟨100⟩ crystallographic fiber texture among the columnar laths which was shown in Fig. 1. A small fraction of smaller grains which formed between the laths revealed distinctly different orientations from the predominant ⟨100⟩ microstructure. Note that colors are assigned based on orientation as it is plotted relative to the deposition direction and a legend is shown in Fig. 2.

3. Experimental procedures

The micro-tensile testing system that was assembled for the current measurements is shown in Fig. 3. The system is based on an original design by sharpe and co-workers [6]. The fixtures and tensile specimens are designed to facilitate alignment and minimize the fixture compliance. The fixtures are mounted on air bearings to minimize friction. A load cell with load range of 67 N and a precision of 0.1 N was used to measure the force, and subsequently stress on the specimen.

The specimen was illuminated by a laser and optical interferometric technique based on Fraunhofer diffraction from a double slit [6]. The interferometric technique was used in the measurement of strain in the specimen. An image acquisition system coupled with an optical microscope was also used to capture the images of gauge displacement between two micro-indentation lines that were scribed onto the specimen. Image correlation techniques were then used to determine the strain distribution in the samples.

The LIGA Ni tensile specimens were shown in Fig. 4. These were loaded to failure in tension at a constant strain rate of 0.00012 s^{-1}. The data from the load cell, optical detectors and image analysis were synchronized and captured using a commercial data acquisition system.

4. Results and discussions

4.1. Stress–strain behavior

The micro-tensile test results obtained for the 200 μm thick structure are plotted in terms of true stress and true

Figure 2 Microtexture of the as-plated LIGA Ni from sulfamate bath.

strain in Fig. 5a. This shows that the plastic deformation starts at very low strain levels (∼0.01). However, because of a machine frame compliance problem, it is very difficult to get accurate measurements of the elastic deformation of the sample. A stiffer load frame/load train design is, therefore, needed to obtain measurements of elastic deformation and the Young's modulus. In this paper, a Young's modulus of 189 GPa is obtained by linear fit of limited data in elastic regime from 50 μm sample test and is used as a material constant in our estimation for 0.2% offset yield stress in other cases. Nevertheless, the ultimate tensile strength measured for the 200 μm sample was 547 MPa. The maximum load that was applied at the onset of sample failure was ∼16 N.

In the case of the 100 μm sample, the stress–stain behavior was similar to that of the 200 μm thick sample (Fig. 5a and b). The ultimate tensile strength of

TABLE II Summary of tensile properties

Thickness (μm foil)	Hardening exponent n	Strength coefficient K (MPa)	0.2% offset yield stress (MPa)	Ultimate tensile stress (MPa)	Plastic elongation to failure
50	0.054	532.6	385	497	6.6%
100	0.113	848.1	475	587	6.2%
200	0.053	637.3	450	547	8.5%

TABLE III Comparison of tensile properties

	Yield stress (MPa)	Ultimate tensile stress (MPa)	Young's modulus (GPa)
Handbook [7]	59	317	207
Mazza *et al.* [8]	∼405	∼782	∼202
Sharpe *et al.* [9]	∼323	∼555	∼176
Xie *et al.* [4]	∼400	∼540	∼175
Christenson *et al.* [2]	∼277	–	∼160

the 100 μm structure was 587 MPa and the maximum load at onset of sample failure was ∼12.7 N. Similarly, as shown in Fig. 5c, early evidence of plastic deformation is apparent in the 50 μm sample. The ultimate tensile strength in this case was 497 MPa and the maximum load at the onset of sample failure is ∼3.9 N. There is, therefore, no evidence of a thickness effect in LIGA Ni MEMS structures with thicknesses between 50 and 200 μm. The tensile properties are summarized in Table II.

Other measurements of the tensile properties of Ni are listed in Table III for easy comparison. Mazza *et al.* [7] reported the yield stress of ∼405 MPa, the ultimate strength of ∼782 MPa and the Young's Modulus of ∼202 MPa. The difference in numbers is probably because the material they were testing has a different microstructure and is obviously stronger. Nevertheless, the values of tensile properties are in fairly good agreement with the work of Sharpe *et al.* [8], Xie *et al.* [4] and Christenson *et al.* [2] for similar columnar microstructure LIGA nickel film.

4.2. Deformation substructures

In order to study the local deformation carefully, an image acquisition system attached to an optical microscope was used to capture the images of the specimen during the test. Image correlation techniques were then used to determine the strain distribution in the samples.

As shown in Fig. 6, deformation substructures of different stages were captured. Two landmarks were made before the test, as shown in Fig. 6a. This can be used in a real time pattern matching process to measure the local strain. Clear surface morphology changes can be seen in Fig. 6b. This is followed by the onset of the instability deformation—necking as shown in Fig. 6c. The sample failed quickly after the onset of necking (Fig. 6d).

The above results suggest that plastic deformation occurs uniformly across the gauge section, prior to the onset of necking (instability), which is associated presumably with the local formation of micro-voids [7].

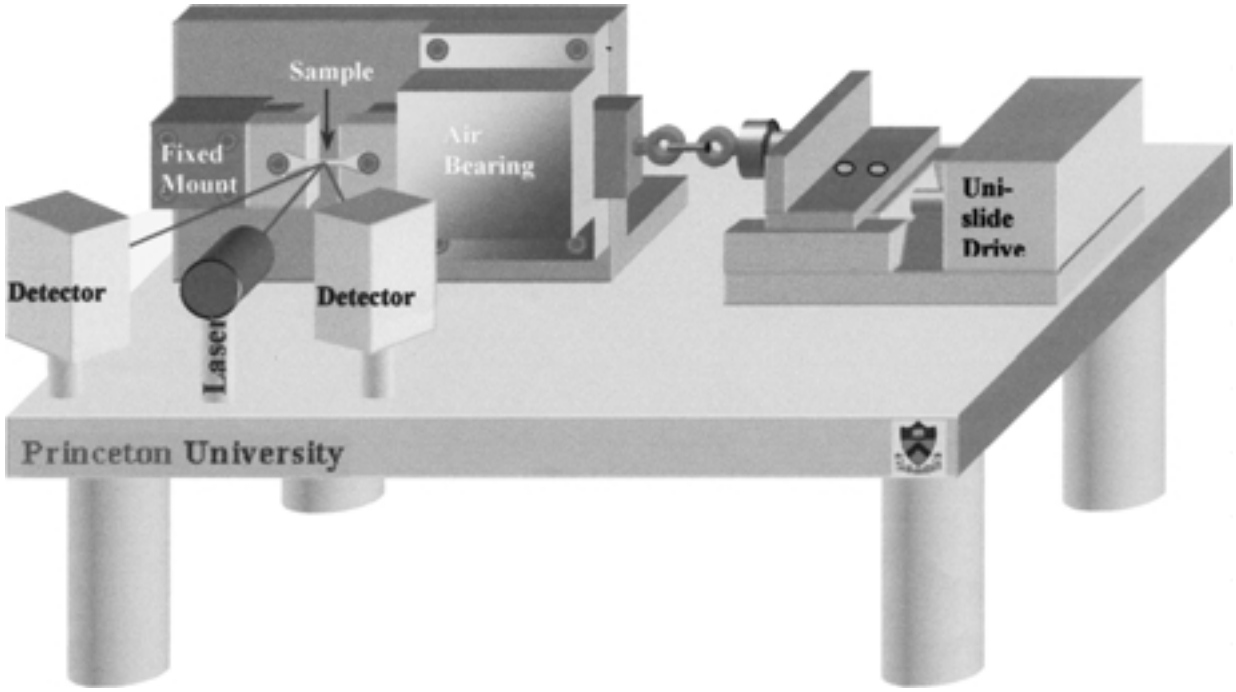

Figure 3 A schematic illustration of the micro-tensile testing system.

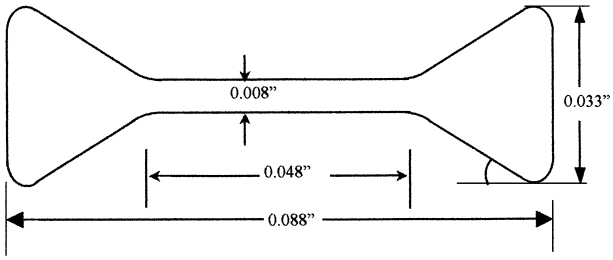

Figure 4 Schematic of the LIGA Ni micro-tensile specimens.

Once this occurs, subsequent deformation occurs rapidly due to the relatively low load machine stiffness.

The results obtained for the above LIGA nickel structures are somewhat different from those obtained for pure Ni foils in earlier studies by Stölken and Evans [8]. In these studies, banded deformation (Fig. 7) was observed in the gauge sections of the foils, even before the onset of necking. The deformation was, therefore, relatively non-uniform in the pure Ni foils that were examined in earlier work [8]. These difference are attributed to the differences between the microstructure and micro-texture of the Ni foils [8] and the current LIGA Ni structure.

4.3. Fracture modes

In all the foils, there was clear evidence of foil necking and final shear fracture at an angle of ∼45° to the loading direction (Fig. 8a–c). Rough transgranular fracture

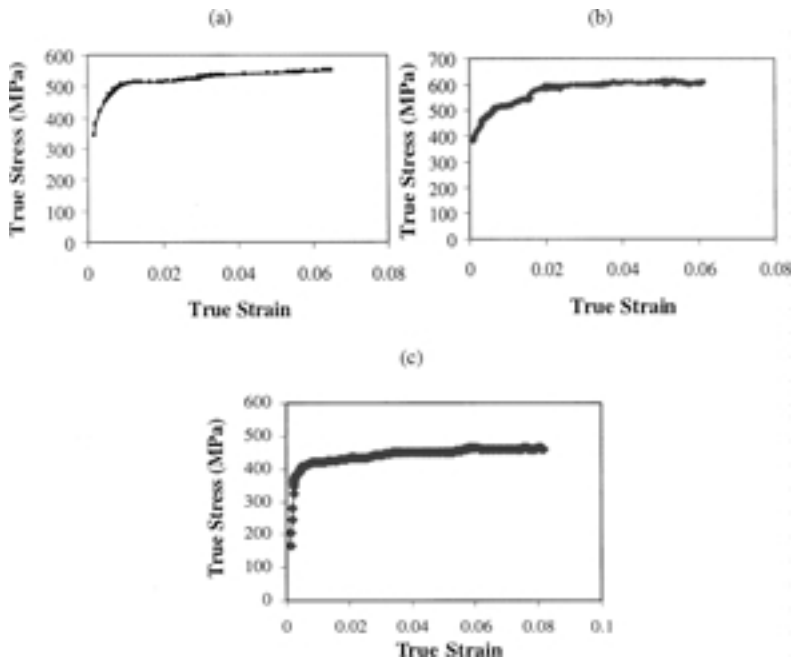

Figure 5 Micro-tensile results of the LIGA Ni sample plated from sulfamate baths with different thickness: (a) 200 μm, (b) 100 μm, and (c) 50 μm.

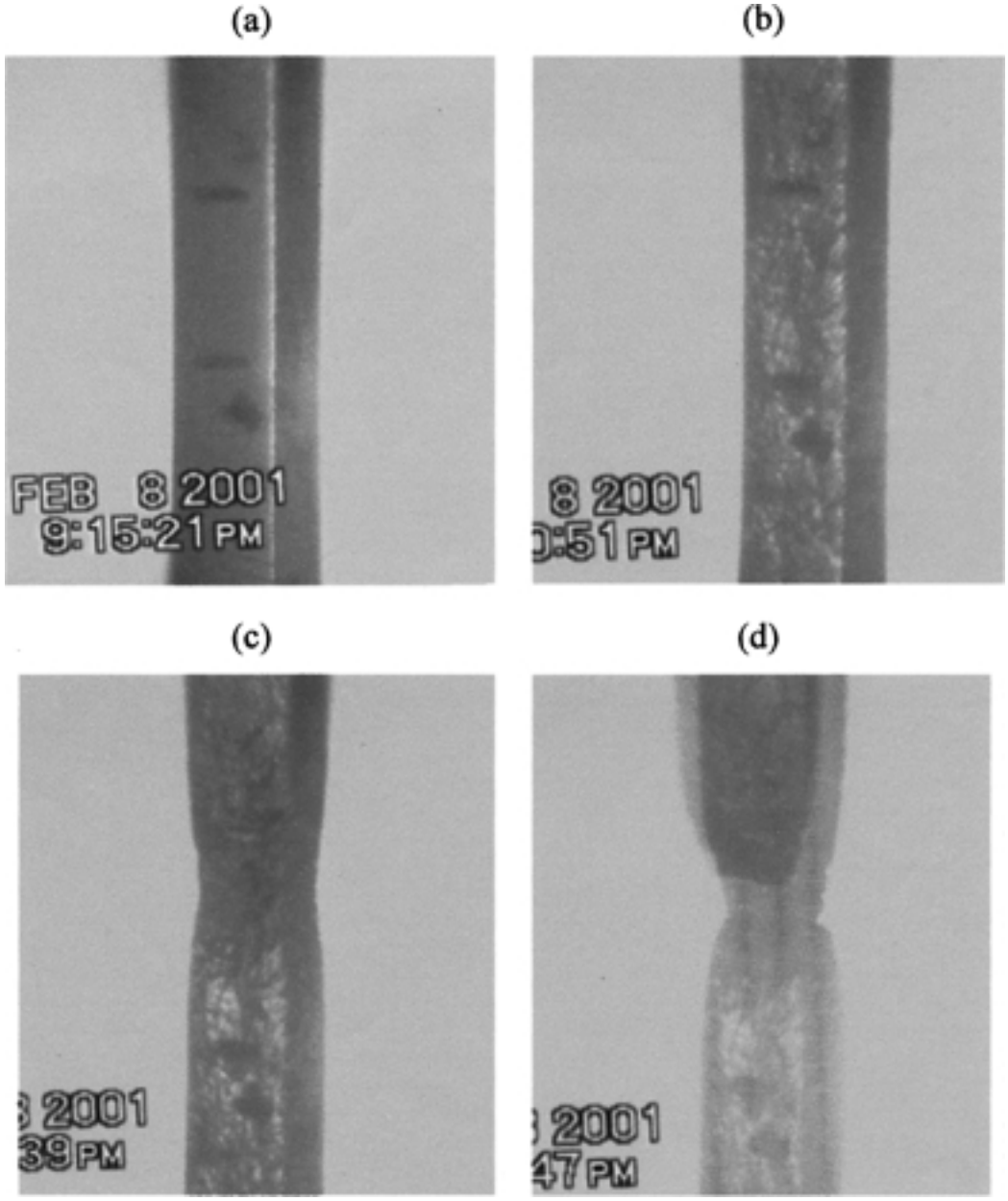

Figure 6 Typical stages in the elastic-plastic deformation: (a) $t = 0$ min 0 sec, (b) $t = 5$ min 51 sec, (c) $t = 6$ min 31 sec, and (d) $t = 6$ min 47 sec.

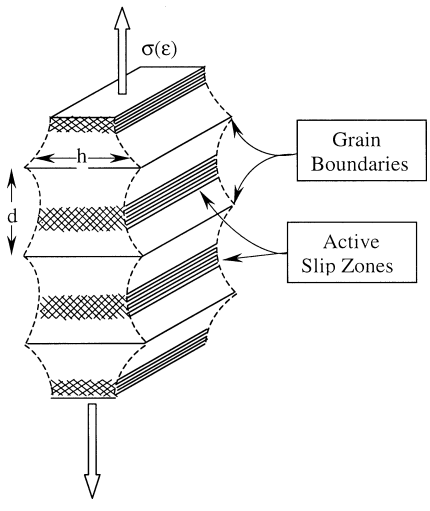

Figure 7 Schematic illustration of banded deformation in Ni foils (taken from Stölken and Evans [11]).

modes were observed in all cases, along with evidence of secondary cracks (Fig. 8a–c). In the case of the 50 μm thick structure, a sharp edge is formed, following the onset of necking and shear fracture (Fig. 8c). However, similar sharp edges were not observed in the thicker samples.

Fracture in 100 and 200 μm thick foils occurs by a combination of faceted fracture and shear fracture. In the case of the 50 μm foil, the formation of sharp edge is presumably a result of combination of necking and cracking along shear planes that are at an angle of $\sim 45^\circ$ to the loading axis.

4.4. Analysis

The uniaxial true stress—true stain behavior of the LIGA nickel MEMS structures can be characterized using the so called Hollomon equation [14], which was

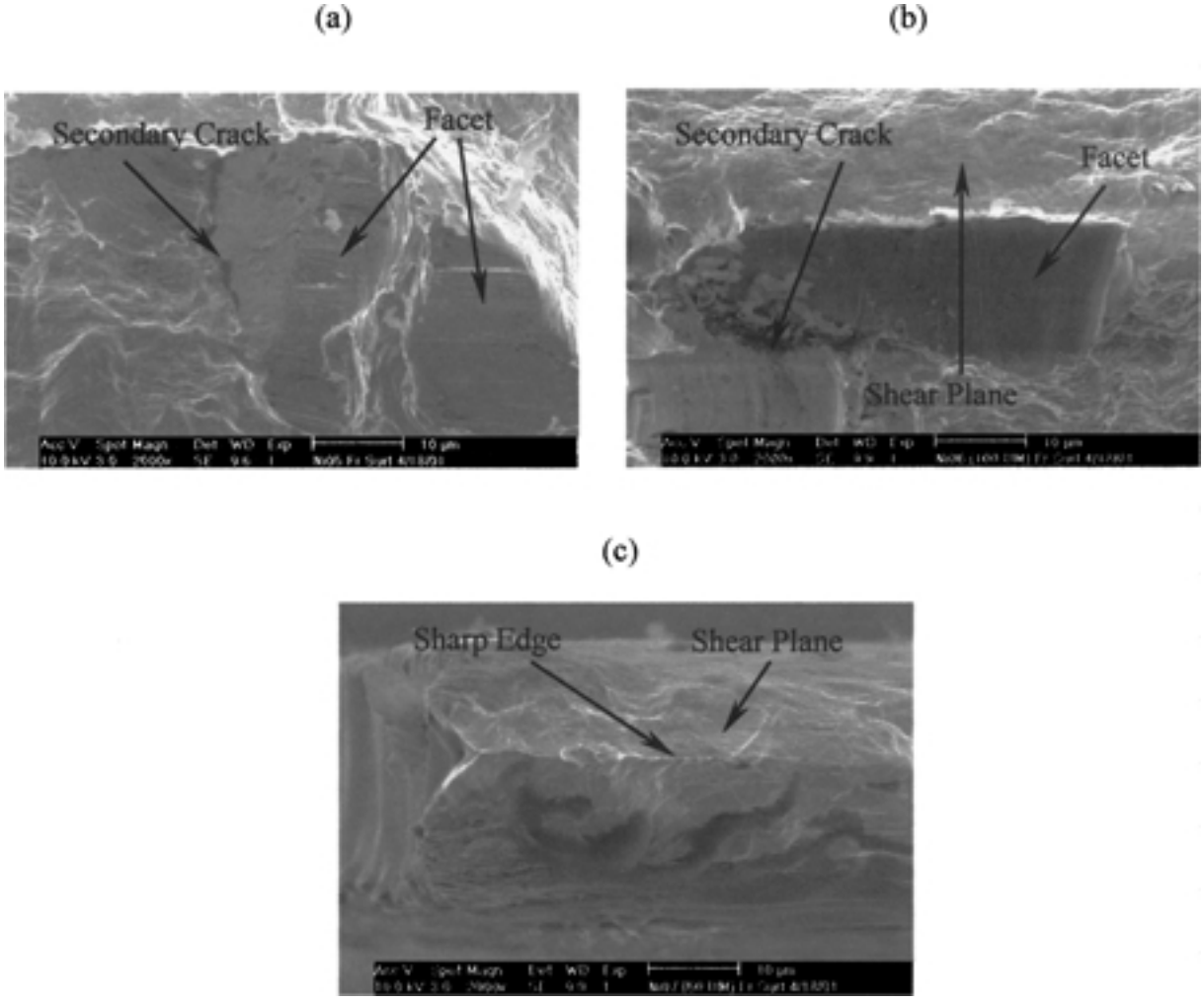

Figure 8 Typical fracture modes obtained from structures with different thickness: (a) 200 μm, (b) 100 μm, and (c) 50 μm.

actually developed by Bülfinger [15] a few hundred years earlier. This gives:

$$\sigma = K\varepsilon^{n} \tag{1}$$

where σ is the true stess, K is a strength coefficient/flow stress corresponding to a strain of unity, ε is the true strain and n is the strain hardening exponent. The strain hardening exponents obtained form the analysis of the measured stress-strain data are presented in Table II along with the basic tensile properties (0.2% offset yield strength, ultimate tensile strength and plastic elongation to failure). In the case of 50 μm sample, the hardening exponent is around 0.054, indicating that there is a very weak hardening effect. Similarly, in 200 μm sample very weak hardening effect is found. The hardening exponent is about $\sim$ 0.053. Interestingly, a stronger hardening effect is found in 100 μm sample with hardening exponent as high as $\sim$0.113.

The absence of a strong thickness effect is not surprising for foils with thicknesses between 50 and 200 μm. This is because local strain gradient plasticity (Fig. 9) and global strain gradient plasticity effects (Fig. 10) are generally considered to be small in Ni foils within the 50–200 μm thickness range [11]. Fig. 9 shows the scenario of the deformation of polycrystals. With the necessary constraint, voids and overlaps can be

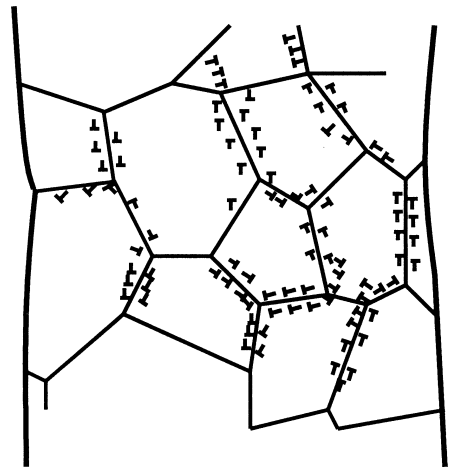

Figure 9 Schematic of local strain gradient plasticity sources (taken from Ashby [12]).

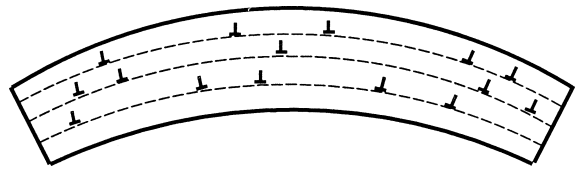

Figure 10 Schematic of global stain gradient plasticity in curved beam (taken from Courtney [10]).

eliminated by the introduction of geometrically necessary dislocations that result from the local strain gradients at the grain boundaries. While in Fig. 10, geometrically change of bending beam is accommodated by the introduction of geometrically necessary dislocations associated with the global strain gradient (generated by the applied bending moment). In our case of the foils, the integrated effects of local strain gradients around grain boundaries (Fig. 9) are relatively small. Also, there are no applied strain gradients under tensile loading. This is in contrast to the strain gradients that are inherent to the deformation of the foils or structures under bending conditions (Fig. 10) [11]. Stölken and Evans [11] and Shrotriya *et al.* [13] have shown that for Micro-bend tests, there is apparent thickness effect on the measurement and they suggested that the micro-bend test method can be used to obtain a composite length-scale parameter, l_c that is primarily associated with rotational gradients. The length-scale is measured to be $\sim$5.3 μm for foils between 25 and 175 μm thick. Please note that because of the way they prepared their sample, Stölken and Evans [11] found some effects of thickness in their tensile experiment that is associated with the different microstructures after the heat treatment of the samples with different thickness. This is eliminated in our study by anneal the sample first then reduces the thickness by TEM sample preparation techniques. Thus, the relatively uniform microstructure minimizes the possible contribution from the variation of local strain gradient around grain boundary while the uniform deformation nature of tensile tests eliminates the contribution from global strain gradient. The limited effects of specimen thickness are, therefore, consistent with the absence of significant contributions from stain gradient plasticity phenomena.

Finally, it is important to discuss the strong evidence of fracture along shear planes (Fig. 8a–c). This is in contrast to bulk Ni that exhibits a Mode I ductile dimpled fracture mode under uniaxial loading conditions [7]. The current results, therefore, suggest that the final fracture occurs by tearing shear planes that are inclined at $\sim$45° to the loading direction. The onset of such tearing begins at the onset of necking and continues until catastrophic failure is initiated in foils with the 100 and 200 μm thickness. The structures neck down to a sharp edge in the case of the 50 μm thick structure.

5. Summary and concluding remarks

1. The LIGA nickel MEMS Structures exhibit a predominantly $\langle 100 \rangle$ crystallographic fiber texture after plating from a sulfamate bath. The as-plated structure also has a columnar structure with an average column height of $\sim$500 nm.

2. Micro-tensile tests have been performed for LIGA Ni samples with 3 different thicknesses (50, 100 and 200 μm). No apparent effect of thickness on the mechanical behavior for LIGA Ni MEMS structure has been found. This is due to the lack of contribution from the strain gradient plasticity phenomena.

3. The measured 0.2% offset yield stress, the ultimate strength and the Young's Modulus are in fairly good agreement with the work done by Mazza *et al.* [8], Sharpe *et al*. [9], Xie *et al.* [4] and Christenson *et al.* [2]. A very weak hardening effect is found for the 50 and 200 μm thick foils with hardening exponent of $\sim$0.05, while 100 μm thick foil exhibits stronger hardening effect with hardening exponent of $\sim$0.11.

4. Fracture in the 50, 100 and 200 μm thick foils occurs by a combination of faceted fracture and transgranular failure. Also, a significant amount of necking is observed in all the three foils. In the case of the 50 μm foil, a sharp edge is formed, presumably as result of cracking along shear planes that are at an angle of $\sim$45° to the loading axis.

Acknowledgements

The research is supported by the Division of Materials Research of The National Science Foundation. Appreciation is extended to the Program Manager, Dr K. Murty for his encouragement and support.

References

1. M. MADOU, "Fundamental of Microfabrication" (CRC Press, Boca Raton, FL, 1999).
2. T. CHRISTENSEN, T. BUCHHEIT, D. T. SCHMALE and R. J. BOURCIER, in "Microelectromechanical Structures for Materials Research," Mechanical and Metallographic Characterization of Nickel and 80%Ni–20%Fe Permalloy, edited by S. Brown et al. (Materials Research Society, 1999) p. 185.
3. H. LAST, K. J. HEMKER and R. WITT, MEMS, in "Materials Science of Microelectromechanical Systems (MEMS) Devices II," Material Microstructure and Elastic Property Modeling, edited by de Boer et al. (Materials Research Society, 2000) p. 191.
4. Z. L. XIE, D. PAN, H. LAST and K. J. HEMKER, in "Materials Science of Microelectromechanical Systems (MEMS) Devices II," Effect of As-Processed and Annealed Microstructures on the Mechanical Properties of LIGA Ni MEMS, edited by de Boer et al. (Materials Research Society, 2000) p. 197.
5. T. E. BUCHHEIT, D. A. LAVAN, J. R. MICHAEL, T. R. CHRINSTENSON and S. D. LEITH, *Metall. Mater. Trans.* **33A** (2002) 539.
6. W. N. SHARPE, B. YUAN, R. VAIDYANATHAN and R. L. EDWARDS, "New Test Structures and Techniques for Measurement of Mechanical Properties of MEMS Materials," in Proc. of the SPIE—The Int. Society for Optical Engineering, Symposium on Microlithography and Metrology in Machining II, 1996, Vol. 2880, p. 78.
7. "Metals Handbook," 10th ed., Vol. 2 (ASM International, 1990).
8. E. MAZZA, S. ABEL and J. DUAL, *Micro Syst. Techn.* **2** (1996) 197.
9. W. N. SHARPE, D. A. LAVAN and R. L. EDWARDS, "Mechanical Properties of LIGA-Deposited Nickel for MEMS Transducers," Transducers 97-1997 International Conference on Solid-State Sensors and Actuators, Digest of Technical Papers, 1997, Vol. 1, p. 607.
10. T. H. COURTNEY, "Mechanical Behavior of Materials" (McGraw Hill, New York, NY, 1990).
11. J. S. STÖLKEN and A. G. EVANS, *Acta Materialia* **46** (1998) 5109.
12. M. F. ASHBY, *Phil. Mag.* **21** (1970) 399.
13. P. SHROTRIYA, S. M. ALLAMEH, J. LOU, T. BUCHEIT and W. O. SOBOYEJO, *Mech. Mater. J.* **35** (2003) 235.
14. J. H. HOLLOMON, *Trans. AIME* **162** (1945) 268.
15. G. B. BÜLFINGER, *Comm. Acad. Petrop.* **4** (1735) 164.